



OPEN

Tropical forest restoration under future climate change

Alexander Koch and Jed O. Kaplan

One of the most promising ways to rapidly remove CO₂ from the atmosphere is through the restoration of tropical forests. Ongoing and future climate change may, however, threaten the permanence of carbon stored through restoration. Excessive heat, drought or increased disturbances such as wildfire could all negatively impact the integrity of restored carbon. To investigate these risks to tropical forest restoration, we performed 221 simulations with a dynamic global vegetation model (LPJ-LMfire) driven by a range of future climate scenarios and ecophysiological responses to CO₂ concentrations. We show that carbon in restored tropical forests is largely preserved under the entire range of potential future climates, regardless of assumptions we make about the potential for CO₂ fertilization of photosynthesis. Restoring even half of the potential area can account for 56–69% of the carbon storage, depending on whether areas are selected for low cost or high carbon gain.

Limiting anthropogenic global warming to less than 2°C requires both a rapid reduction in greenhouse gas emissions and probably additional drawdown of carbon from the atmosphere¹. Preserving and restoring the tropics' rich forest carbon stocks is a valuable tool for this task, as it delivers a carbon benefit that is less attenuated by climate responses to increased tree cover (albedo warming) compared to high latitudes^{2,3}. If undertaken following best practices, restoration also brings benefits to biodiversity and communities living in and around tropical forests⁴. Currently, most estimates of the potential of tropical forests as a carbon sequestration mechanism are based on present-day climate and do not take into account potential impacts from future climate change and rising atmospheric CO₂ concentrations^{2,3,5,6}, or only scale carbon uptake to temperature and CO₂^{7,8}. Forest restoration projects, however, are also vulnerable to detrimental impacts from climate change; rising temperatures, drought, insect outbreaks and increases in wildfire threaten the success of these projects and their aim to store carbon in biomass and soils over the entire project lifetime of 50 to over 100 years, that is, permanently^{9,10}. Failure of permanence in restoration projects can lead to habitat and monetary losses, and may result in additional carbon emissions if the project was part of an emissions offsetting scheme. While old-growth humid tropical forests have a high resilience to disturbance, carbon storage in the seasonally arid tropics is at risk if turnover times decrease due to disturbances¹¹. A recent qualitative assessment suggested that fire and drought will affect ecosystems in all parts of the tropics in the future⁹. These risks to the permanence of tropical forest restoration are poorly understood, particularly when considering the interplay between climate and atmospheric CO₂, and their influence on vegetation productivity and disturbance.

Here we assess the impact of future climate change, atmospheric CO₂ concentrations and lightning-caused wildfires on forest restoration efforts in the tropics by conducting 221 dynamic global vegetation model (DGVM) simulations that cover the full range of available climate change scenarios and varying degrees of future CO₂ fertilization on photosynthesis. We use the LPJ-LMfire DGVM to simulate above- and below-ground biomass accumulation for the period 2020–2100 from restoring non-crop-producing agricultural land based on a published restoration opportunity map². LPJ-LMfire

performs reasonably well against observations of present-day tropical biomass carbon and is comparable to other DGVMs in its productivity response to rising CO₂ temperature and drought, while its carbon accumulation rate is on the upper end of observation-based estimates. Because it is unlikely that all of the potential area available for tropical forest restoration could be realized, we also select half of the restoration area based on present-day carbon uptake potential, cost, or both, as well as accounting for climate change resilience by selecting for year 2100 carbon uptake potential.

Climate impact on carbon stored in restored tropical forest

Restoring 128 Mha (11%) of the tropical non-crop-producing areas (classified as 'pasture' in land use datasets) to tropical forest results in a cumulative carbon (above and below ground, including soil carbon) uptake of 24.1–39.6 PgC between 2020 and 2100, depending on the severity of future climate change, the degree of potential future CO₂ fertilization, and whether the effects of wildfire are taken into account (Fig. 1). Under the 'default case' where potential future CO₂ fertilization in vegetation, climate change and wildfire are ignored—this is what is commonly used to assess the mitigation potential of nature-based solutions—cumulative carbon accumulation from restoration is 28.5 PgC (range 25.0–29.6 PgC) by 2100. Carbon storage from restoration increases under all climate change scenarios, regardless of whether CO₂ fertilization is included or not, and in 92% of the simulations, carbon continues to accumulate until the end of the century. Carbon accumulation into restoration is strongest at the end of the expansion in restoration area (2030) and declines thereafter, more so when CO₂ fertilization is not included (Extended Data Fig. 1).

In the unconstrained CO₂ fertilization experiment (CO_{2-free}), the impacts of atmospheric CO₂ and climate change cause carbon storage to increase by 2100 in the order of projected atmospheric CO₂ concentrations in the Shared Socio-economic Pathways (SSPs) future scenarios. Carbon storage is lowest in the low-CO₂ SSP1-26 scenario (23.4% increase relative to the default case; range 0.5–44.5%) and highest in the high-CO₂ scenario SSP5-85 (39.4%; 26.6–67.7%), with carbon storage in the SSP2-45 and SSP3-70 scenarios being in between. This picture is reversed in the limited CO₂

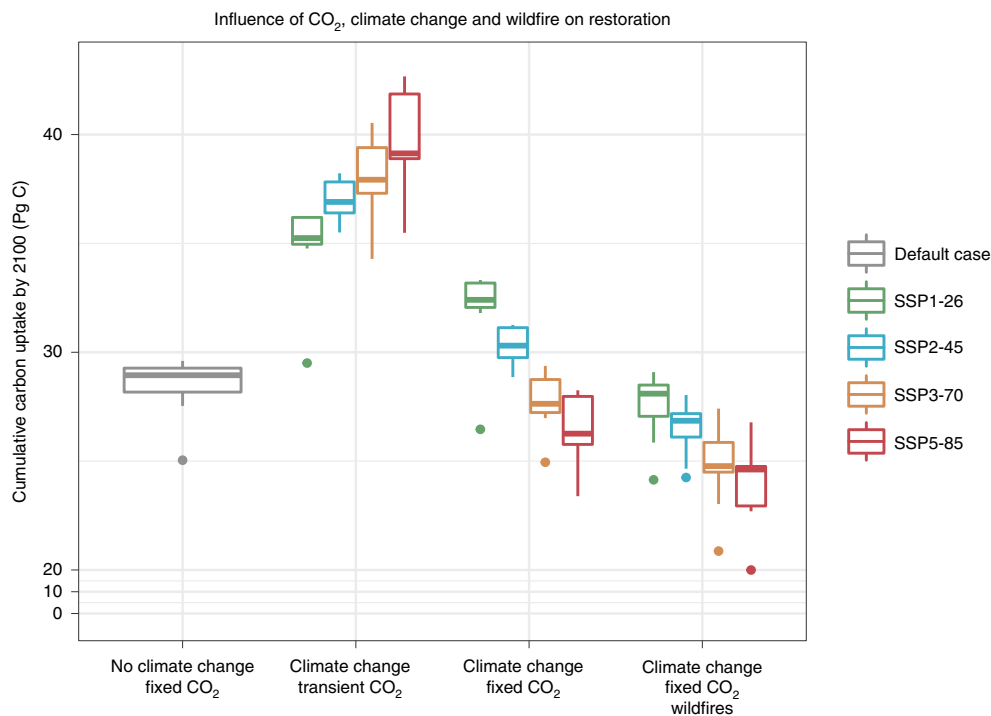


Fig. 1 | Influence of potential CO₂ fertilization, climate change and wildfire on carbon storage by tropical forest restoration (2020–2100). The ‘default case’ without climate change and CO₂ fertilization, different climate change scenarios (SSPs) with unconstrained or limited CO₂ fertilization, and wildfire are shown. Each sample is based on the climate of one potential realization of an SSP scenario simulated by one of 13 CMIP6 models. Boxplots represent 25th, 50th and 75th quantiles, whiskers are the 5th and 95th quantiles, and individual points are outliers. Note the nonlinear y axis (0–20 Pg C). See Extended Data Fig. 2 for a spatial distribution of carbon gain under SSP2-45 CO₂₂₀₁₄ and wildfire.

fertilization experiment (CO₂₂₀₁₄), where we assume that CO₂ fertilization will not take place in the future by keeping atmospheric CO₂ concentrations constant at 2014 levels (399 ppm) and any difference in carbon storage between the SSP scenarios is caused solely by differences in projected future climate change. Here carbon storage at 2100 is most reduced relative to the default case under SSP5-85 (−7.3%; −16.5 to 11.7%) and least reduced under SSP1-26 (13.1%; −9.8 to 32.5%), with the other two SSPs being in between. When including the impact of wildfires in CO₂₂₀₁₄, carbon storage is further reduced relative to the default case, depending on the SSP scenario—between −15.1% (−27.4 to 1.7%) in SSP5-85 and −3.0% (−17.7 to 9.6%) in SSP1-26.

The contribution of each factor—CO₂ fertilization, climate change and wildfires—to changes in carbon storage potential varies strongly between SSPs, with CO₂ fertilization having the largest contribution under high-CO₂ scenarios (for example, 42.0% relative to the default case under SSP5-85), and climate change having the greatest contribution (14.6% relative to the default case under SSP1-26) under scenarios with relatively low CO₂ concentrations. Wildfires contribute 10.6–14.1% to changes in carbon storage (Extended Data Fig. 3).

Prioritization of forest restoration

Restoring all potential tropical forest area is probably not feasible for multiple reasons, including political, economic and social challenges. We therefore consider a scenario where only half of the potential restoration area (64 Mha) is realized. In selecting which half to restore from the default case, we explore scenarios prioritized for either carbon uptake potential, opportunity cost of restoring land over using it for agriculture, that is, the waived revenue from agricultural activity when restoring land, or both carbon and cost combined. Selecting individual grid cells for carbon uptake potential

yields the highest carbon storage, achieving 68.9% of the carbon gained by restoring all available land, while selecting to minimize opportunity cost yields the lowest carbon storage but still represents more than half (56.4%) of the full restoration capacity (Fig. 2a; grey dashed lines). Meanwhile, selecting for both carbon uptake potential and opportunity costs results in a cumulative carbon uptake by 2100 close to the scenario that solely maximizes carbon uptake potential.

The impact of climate change and potential CO₂ fertilization increases average carbon storage on all prioritization scenarios for the previously selected locations, with the smallest gains under SSP1-26 and the largest gains under SSP5-85 (Fig. 2a). The largest gains in carbon storage relative to its respective default case are found in the low-cost scenario, probably because CO₂ fertilization increases productivity on marginal lands that currently have low agricultural value (Extended Data Fig. 3). Without CO₂ fertilization, carbon storage is lower than under default conditions in all prioritization scenarios and follows the severity of climate change in the SSPs, with the smallest reductions under SSP1-26 and the largest reductions under SSP5-85 (Fig. 2a). Gains in carbon storage relative to its default case are lowest in the scenario where we mask for carbon uptake potential, as regions with higher carbon densities and more vegetation have more carbon to lose under climate change than marginal lands.

By selecting locations where the impact of climate change is minimized, all scenarios show increases in carbon storage relative to the default case where the selection of restoration sites is made only on the basis of present-day conditions (Fig. 2b). This occurs regardless of the degree of potential future CO₂ fertilization. Here the increase in carbon storage relative to the prioritization based on present-day conditions is greatest when selecting for carbon uptake potential, and smallest when selecting for cost, probably due to the previously stated carbon density–carbon loss relationship.

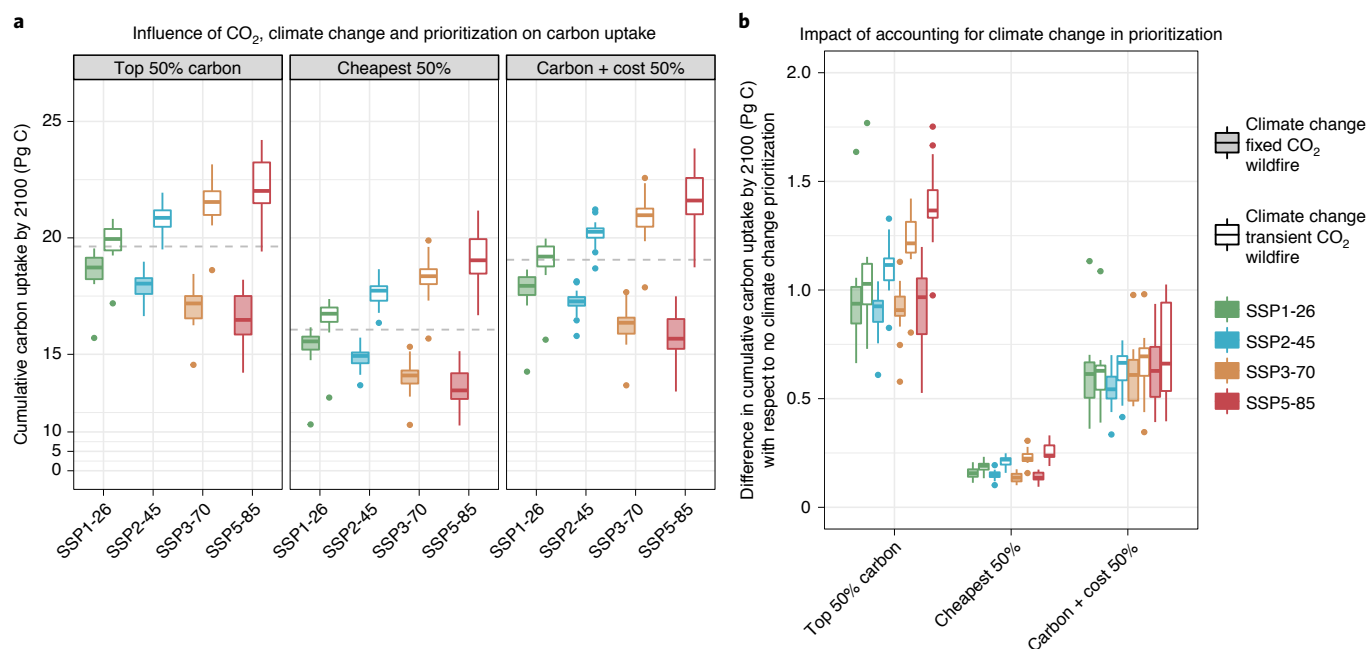


Fig. 2 | Impact of different prioritization strategies on the effects of CO₂ fertilization and climate change on carbon storage in tropical restoration areas by 2100. **a**, Above- and below-ground carbon storage in CO_{2,free} (transparent boxplots) and CO_{2,2014} (filled boxplots) following the prioritization of half the restoration area by targeting the highest carbon uptake potential ('top 50% carbon'), lowest opportunity cost ('cheapest 50%') and highest carbon uptake combined with lowest cost ('carbon + cost 50%') based on the carbon uptake under default conditions, that is, no climate change and fixed CO₂. **b**, Effect of including effects of climate change in prioritization on carbon storage relative to prioritization in **a**. Grey dashed lines in **a** represent the mean carbon storage under default conditions after prioritization. Each sample is based on the climate of one potential realization of an SSP scenario simulated by one of 13 CMIP6 models. Boxplots represent 25th, 50th and 75th quantiles, whiskers are the 5th and 95th quantiles, and individual points are outliers. Note the nonlinear y axis in **a** (0–20 Pg C).

Restoration opportunities

Finally, we combine climate change and wildfire threats to carbon storage with the opportunity cost of land to create a restoration opportunity index that indicates which restoration areas have the most cost-effective long-term (2030–2100) carbon storage potential for all climate change scenarios in CO_{2,2014}. Between 5% (SSP5-85) and 7% (SSP1-26) of the 128 Mha of the restored area has a high (>0.75) restoration opportunity index, meaning these regions can retain carbon until at least 2100 and are cost-effective to restore (Supplementary Table 1). Under the intermediate SSP2-45 scenario, 6% of the restoration area has a high restoration opportunity index, with central Africa and the island of New Guinea being most suitable from a climate change and cost perspective (Fig. 3). Generally, under all SSPs, northwestern South America, West and Central Africa, the maritime continent and parts of Southeast Asia are promising for restoration, while southwestern Brazil, India and other parts of Southeast Asia (for example, south China) face the greatest climate change and cost barriers to restoration (Supplementary Fig. 1).

Our modelling experiments show that restoration of tropical forests over a relatively small area, 11% of the non-crop-producing agricultural area of the tropics, has the potential to sequester 2–4 years of today's worth of anthropogenic carbon emissions over multiple decades. Most of this carbon is preserved at least until the end of the century under a range of future atmospheric CO₂ concentrations and climate change scenarios, independent of the climate model. Despite this relatively small uptake, these results are promising, especially if there would otherwise be no restoration, meaning no or very little additional carbon uptake. However, it is also important to recognize uncertainties and limitations in our experimental design. Because we made a very large number of simulations, we could use

only one vegetation model (LPJ-LMfire). DGVMs vary substantially in their response to future climate and atmospheric CO₂ concentrations¹², and in their representation of productivity and mortality processes^{13–15}, meaning these differences can only be captured by conducting all experiments with a large set of models. Thus, it is important to consider the representativeness of LPJ-LMfire relative to other DGVMs to extract any policy-relevant information. Furthermore, biogeophysical land–atmosphere climate feedbacks that we did not consider could have the potential to either amplify or attenuate the carbon storage from restoration. In the following sections, we discuss each of these issues in further detail.

Representativeness of LPJ-LMfire

We evaluated LPJ-LMfire against observations and an ensemble of DGVMs (TRENDYv9, $n=9$) participating in the Global Carbon Budget effort¹⁶ and show that LPJ-LMfire is representative, that is, not an outlier, in its representation of biomass, productivity, and climate and CO₂ sensitivities of the current generation of DGVMs (see Supplementary Information). The productivity and biomass responses in LPJ-LMfire to drought and heat extremes (for example, during El Niño events in central Amazonia) are also representative of the TRENDY ensemble (Supplementary Fig. 11).

While recruitment at the germination or seedling stage may fail in restoration projects for multiple reasons, both climatic and socio-economic¹⁷, we make the optimistic assumption that, considering the substantial investment in money and labour that will go into large-scale restoration projects, active forest restoration efforts will follow best practices to ensure successful recruitment. Furthermore, recruitment is climate dependent in LPJ-LMfire, and under unfavourable climatic conditions (for example, drought), establishment of new saplings will fail in our model simulations.

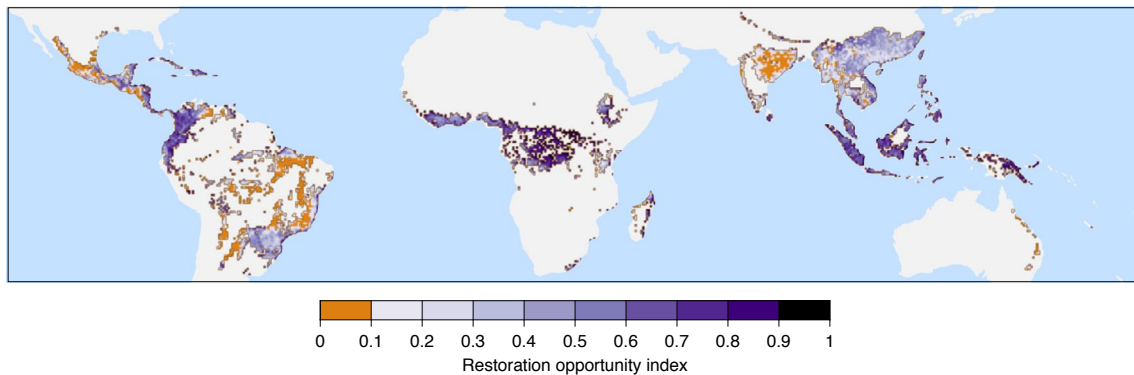


Fig. 3 | Restoration opportunity index. The restoration opportunity index indicates which restoration areas have the most cost-effective long-term (2020–2100) carbon storage potential for all climate change scenarios without additional CO₂ fertilization. It is calculated using the rank sum of carbon and opportunity cost, masked to grid cells with a gain in above- and below-ground carbon over 2030–2100, and stable above- and below-ground carbon storage with no reductions in carbon of more than 10% of the detrended long-term (2030–2100) mean. A score of 1 means that the restoration opportunity index is 1 under all future climate model simulations. This map is for the SSP2-45 CO₂₂₀₁₄ experiment; restoration opportunity index maps for the other scenarios are shown in the Supplementary Information. For maps of carbon gain under SSP2-45 CO₂₂₀₁₄ and opportunity costs, see Extended Data Figs. 2 and 4, respectively.

Uncertainties in fire impacts on restoration

We limit our analysis to wildfire caused by lightning and do not consider anthropogenic ignitions. While this could underestimate the impact of fire on the carbon uptake potential from restoration, we assume that in restoration areas where substantial financial investments are made in promoting long-term carbon uptake and storage, anthropogenic fire would be discouraged through both prohibition on ignitions and passive mitigation such as firebreaks. The omission of anthropogenic ignitions in our simulations precludes equivalent comparison of our simulated burned area with available satellite observations that do not distinguish between anthropogenic and lightning-caused fire¹⁸. In general, the omission of natural fire would overestimate simulated biomass in the seasonally dry tropics (Supplementary Fig. 4), yet on a more local scale, a previous comparison of fires from satellite observation with modelled fire from LPJ-LMfire in areas with little human impact suggests that the model overestimates burned area in the southeastern Amazon Basin by ~20% because the model underestimates fuel moisture under shaded tree canopy during the dry season¹⁹. This means that, presumably, LPJ-LMfire may overestimate the impact of fire on restored tropical forest, particularly in regions with high seasonality in precipitation.

Uncertainties in climate feedbacks

In our experiments, land cover is not coupled with the atmosphere, meaning that land cover change through restoration does not feed back to local climate, and the increased land carbon sink from restoration has no impact on the atmospheric CO₂ used in either the vegetation or climate models. Climate simulated by the sixth Coupled Model Intercomparison Project (CMIP6) models that are used to drive the DGVM simulations is influenced by the biogeophysical properties of the land cover before restoration takes place (that is, grassland), yet land cover change towards more tree cover (for example, through restoration) would probably lead to localized cooling in the tropics^{20,21}. Compared to the simulations with standard CMIP6 general circulation model (GCM) climate, this localized cooling would marginally increase carbon uptake in our simulations (up to 0.13 Pg C; see Supplementary Information), as it reduces the negative carbon response to increasing temperature by attenuating heterotrophic respiration¹².

Uncertainties in the Earth system response

Increased carbon uptake from restoration reduces atmospheric CO₂ concentrations, which in turn leads to less CO₂ fertilization

of the regrowing vegetation and a reduction in carbon uptake by that vegetation²². In CO₂_{free}, CO₂ fertilization follows the prescribed atmospheric CO₂ concentrations of the SSPs and is not reduced by any increased carbon uptake from restoration, meaning the carbon uptake in CO₂_{free} is probably an overestimate. However, since our experiment with no future CO₂ fertilization (CO₂₂₀₁₄) effectively simulates growth conditions as if other limiting factors (climate, nutrients) control plant growth during the 2020–2100 period and thus provides a lower bound on carbon uptake, we capture the full range of the carbon uptake potential from tropical forest restoration. Furthermore, the actual reduction in atmospheric CO₂ would be less than the increase in biomass carbon implied by restoration alone due to the negative response in carbon uptake by oceans and vegetation elsewhere under lower atmospheric CO₂^{22–24}.

While our experiment only considers the carbon uptake potential from tropical restoration, and the impact future climate change may have on these efforts, other parts of the Earth system would also be affected by climate change. For example, the observed carbon sink from intact tropical forests in Amazonia and Africa has recently saturated and is projected to decline under future climate change^{25,26}. This would counteract some of the gain in carbon sequestration through forest restoration. Furthermore, it is important to note that our results by design do not represent estimates of carbon uptake from restoration under each of the SSP storylines, that is, their land use trajectories and atmospheric CO₂ concentrations, but rather show the impact of potential future CO₂ concentrations and climate change scenarios on tropical forest restoration. Therefore, the absence of any Earth system responses to tropical restoration may overestimate the net carbon benefit from tropical forest restoration.

Comparison with other restoration estimates

Our default case estimate of above- and below-ground carbon uptake from restoration over the period 2020–2050 is at the higher end of other independent estimates. Without future climate change and CO₂ fertilization, we simulate an uptake of 0.77 Pg C yr⁻¹ (range 0.73–0.79 Pg C yr⁻¹), compared with 0.53 Pg C yr⁻¹ from a recent observation-based estimate of above- and below-ground carbon sequestration potential scaled to our restoration area⁶. This difference is driven by approximately 50% higher simulated uptake rates in northern South America and south China in LPJ-LMfire, while underestimating uptake rates in southeastern Brazil by on average 31% (Supplementary Fig. 13)⁶. Elsewhere our estimates agree well

with the observation-based spatial distribution of potential carbon uptake; nevertheless, the higher-than-observed carbon accumulation rates present an uncertainty and limitation of our study. Other estimates generally only report annual above-ground carbon accumulation rates and therefore are not directly comparable to our results, for example, refs. ^{3,5,7,8}.

We find that prioritization increases carbon storage by 18%, which is less than the threefold increase found by a recent global study²⁷, probably because we focus on tropical restoration opportunities where differences in carbon storage are less pronounced than elsewhere. Accounting for the impacts of climate change on carbon storage in the prioritization can mitigate only up to 5% of the reductions in carbon storage due to climate change, yet the actual area restored, and ultimately also the resulting carbon uptake, depend on a variety of economic and sociopolitical factors^{3,7,27,28}.

Reductions in carbon uptake are not the only consequence of disturbance events. Repeated fire in particular may destroy seed banks, causing regeneration failure²⁹, while heat and drought stress weaken vegetation, making plants more susceptible to pathogens and insect outbreaks³⁰. Measures to ensure resilience and maintain productivity under climate change, such as planting of drought-tolerant species or nurturing a diverse plant community³¹, are not explicitly included in our simulations, hence again our calculations may represent conservative estimates of what could be possible with careful management. For example, after a super-typhoon, monoculture plantations in Hong Kong were heavily damaged compared with naturally recovering vegetation, and early-successional forest (<39 years) was found to be less resilient than older forest, which was exacerbated by a lower plant diversity in the regrowing vegetation³². Future work will need to go beyond assessing climate change impacts on carbon to also consider climate change impacts on restoring biodiversity³³, as well as the socioeconomic drivers that may threaten the success of restoration activities¹⁷.

Our modelling shows that carbon stored by tropical forest restoration is largely permanent, that is, removed from the atmosphere for at least 80 years. We conclude that while future climate change impacts probably reduce potential carbon sequestration, tropical forest restoration can still play an important part as one of multiple solutions in reducing atmospheric CO₂ concentrations.

Online content

Any methods, additional references, Nature Research reporting summaries, source data, extended data, supplementary information, acknowledgements, peer review information; details of author contributions and competing interests; and statements of data and code availability are available at <https://doi.org/10.1038/s41558-022-01289-6>.

Received: 6 August 2021; Accepted: 14 January 2022;

Published online: 17 February 2022

References

- Rogelj, J. et al. in *Special Report on Global Warming of 1.5°C* (eds Masson-Delmotte, V. et al.) Ch. 2 (IPCC, 2019).
- Griscom, B. W. et al. Natural climate solutions. *Proc. Natl Acad. Sci. USA* **114**, 11645–11650 (2017).
- Griscom, B. W. et al. National mitigation potential from natural climate solutions in the tropics. *Phil. Trans. R. Soc. B* **375**, 20190126 (2020).
- Seddon, N. et al. Understanding the value and limits of nature-based solutions to climate change and other global challenges. *Phil. Trans. R. Soc. B* **375**, 20190120 (2020).
- Busch, J. et al. Potential for low-cost carbon dioxide removal through tropical reforestation. *Nat. Clim. Change* **9**, 463–466 (2019).
- Cook-Patton, S. C. et al. Mapping carbon accumulation potential from global natural forest regrowth. *Nature* **585**, 545–550 (2020).
- Bastin, J.-F. et al. The global tree restoration potential. *Science* **365**, 76–79 (2020).

- Lewis, S. L., Wheeler, C. E., Mitchard, E. T. A. & Koch, A. Restoring natural forests is the best way to remove atmospheric carbon. *Nature* **568**, 25–28 (2019).
- Seidl, R. et al. Forest disturbances under climate change. *Nat. Clim. Change* **7**, 395–402 (2017).
- Anderegg, W. R. L. et al. Climate-driven risks to the climate mitigation potential of forests. *Science* **368**, eaaz7005 (2020).
- Pugh, T. A. M., Arneeth, A., Kautz, M., Poulter, B. & Smith, B. Important role of forest disturbances in the global biomass turnover and carbon sinks. *Nat. Geosci.* **12**, 730–735 (2019).
- Piao, S. et al. Evaluation of terrestrial carbon cycle models for their response to climate variability and to CO₂ trends. *Glob. Change Biol.* **19**, 2117–2132 (2013).
- Friend, A. D. et al. Carbon residence time dominates uncertainty in terrestrial vegetation responses to future climate and atmospheric CO₂. *Proc. Natl Acad. Sci. USA* **111**, 3280–3285 (2014).
- Fleischer, K. et al. Amazon forest response to CO₂ fertilization dependent on plant phosphorus acquisition. *Nat. Geosci.* **12**, 736–741 (2019).
- Terrer, C. et al. Nitrogen and phosphorus constrain the CO₂ fertilization of global plant biomass. *Nat. Clim. Change* **9**, 684–689 (2019).
- Friedlingstein, P. et al. Global carbon budget 2020. *Earth Syst. Sci. Data* **12**, 3269–3340 (2020).
- Coleman, E. A. et al. Limited effects of tree planting on forest canopy cover and rural livelihoods in northern India. *Nat. Sustain.* **4**, 997–1004 (2021).
- van der Werf, G. R. et al. Global fire emissions estimates during 1997–2016. *Earth Syst. Sci. Data* **9**, 697–720 (2017).
- Pfeiffer, M., Spessa, A. & Kaplan, J. O. A model for global biomass burning in preindustrial time: LPJ-LMfire (v1.0). *Geosci. Model Dev.* **6**, 643–685 (2013).
- Bonan, G. B. Forests and climate change: forcings, feedbacks, and the climate benefits of forests. *Science* **320**, 1444–1449 (2008).
- Li, Y. et al. Potential and actual impacts of deforestation and afforestation on land surface temperature: impacts of forest change on temperature. *J. Geophys. Res. Atmos.* **121**, 14372–14386 (2016).
- Koch, A., Brierley, C. & Lewis, S. L. Effects of Earth system feedbacks on the potential mitigation of large-scale tropical forest restoration. *Biogeosciences* **18**, 2627–2647 (2021).
- Jones, C. D. et al. Simulating the Earth system response to negative emissions. *Environ. Res. Lett.* **11**, 095012 (2016).
- Krause, A. et al. Large uncertainty in carbon uptake potential of land-based climate-change mitigation efforts. *Glob. Change Biol.* **24**, 3025–3038 (2018).
- Brienen, R. J. W. et al. Long-term decline of the Amazon carbon sink. *Nature* **519**, 344–348 (2015).
- Hubau, W. et al. Asynchronous carbon sink saturation in African and Amazonian tropical forests. *Nature* **579**, 80–87 (2020).
- Strassburg, B. B. N. et al. Global priority areas for ecosystem restoration. *Nature* **586**, 724–729 (2020).
- Zeng, Y. et al. Economic and social constraints on reforestation for climate mitigation in Southeast Asia. *Nat. Clim. Change* **10**, 842–844 (2020).
- Flores, B. M. & Holmgren, M. Why forest fails to recover after repeated wildfires in Amazonian floodplains? Experimental evidence on tree recruitment limitation. *J. Ecol.* **109**, 3473–3486 (2021).
- Gely, C., Laurance, S. G. & Stork, N. E. How do herbivorous insects respond to drought stress in trees? *Biol. Rev.* **95**, 434–448 (2020).
- Schnabel, F. et al. Drivers of productivity and its temporal stability in a tropical tree diversity experiment. *Glob. Change Biol.* **25**, 4257–4272 (2019).
- Abbas, S., Nichol, J. E., Fischer, G. A., Wong, M. S. & Irteza, S. M. Impact assessment of a super-typhoon on Hong Kong's secondary vegetation and recommendations for restoration of resilience in the forest succession. *Agric. For. Meteorol.* **280**, 107784 (2020).
- Pecl, G. T. et al. Biodiversity redistribution under climate change: impacts on ecosystems and human well-being. *Science* **355**, eaai9214 (2017).

Publisher's note Springer Nature remains neutral with regard to jurisdictional claims in published maps and institutional affiliations.



Open Access This article is licensed under a Creative Commons Attribution 4.0 International License, which permits use, sharing, adaptation, distribution and reproduction in any medium or format, as long as you give appropriate credit to the original author(s) and the source, provide a link to the Creative Commons license, and indicate if changes were made. The images or other third party material in this article are included in the article's Creative Commons license, unless indicated otherwise in a credit line to the material. If material is not included in the article's Creative Commons license and your intended use is not permitted by statutory regulation or exceeds the permitted use, you will need to obtain permission directly from the copyright holder. To view a copy of this license, visit <http://creativecommons.org/licenses/by/4.0/>.

© The Author(s) 2022

Methods

Tropical forest restoration area. To determine the geographic distribution of land available for tropical forest restoration, we used a widely applied global forest restoration map². This dataset limits potential restoration area to regions that are biogeographically suitable for forest, and excludes croplands. To define the tropics, we masked the potential restoration map with the following three ecoregions from the Ecoregions2017 vegetation map³⁴: ‘Tropical and Subtropical Moist Broadleaf Forests’, ‘Tropical and Subtropical Dry Broadleaf Forests’, and ‘Tropical and Subtropical Coniferous Forests’. The resulting restoration mask includes all tropical and subtropical forest ecoregions with some that are outside the tropical latitudes, but excludes wetlands and high mountain areas (Extended Data Fig. 4). The restoration mask was converted from a presence–absence raster at its native ~350 m resolution to a 0.5° geographical grid by aggregating to the fraction of each 0.5° grid cell available for restoration. Any uncertainties in the allocation of restorable area, distinguishing crop and pasture, and forest to non-forest classification from the original forest restoration map were also implicitly included in our restoration extent. While the resulting restoration area is relatively small, its spatial distribution is representative for most of the humid tropics.

To prioritize for carbon uptake capacity, we selected all grid cells with restoration area greater than 1 ha and ranked these by carbon storage density (above ground and below ground; g m^{-2}) at 2100 under the default scenario. We then selected the top n grid cells with greatest carbon density until cumulatively 64 Mha of restored area was reached. Similarly, for cost we calculated the restoration cost for each grid cell following ref.²⁷ and sorted the grid cells by their cost, beginning with the lowest value, until 64 Mha were reached. To consider the combined impact of carbon uptake and restoration costs, we divided our restoration cost layer by the total carbon uptake per grid cell from restoration and ranked the cost per carbon uptake from cheapest to most expensive, selecting the n grid cells with the lowest values until 64 Mha were reached. We then used the selected grid cells to mask carbon uptake under the various climate change and CO_2 fertilization scenarios. To factor in climate change in the prioritization process, we used the same restoration cost layer but used the carbon density and total carbon uptake layers with climate change impacts in CO_2_{2014} for the year 2100.

Vegetation model. We used the LPJ-LMfire DGVM¹⁹, a version of the Lund-Potsdam-Jena DGVM (LPJ)³⁵. LPJ-LMfire is driven by gridded fields of climate, soil texture and topography at 0.5° resolution, and with a time series of atmospheric CO_2 concentrations (see Supplementary Information). To simulate land use, LPJ-LMfire separates grid cells into fractional tiles of ‘unmanaged’ land that has never been under land use, ‘managed’ land, and areas ‘recovering’ from land use³⁶. Restoration removes land from the ‘managed’ tile and transfers it to the ‘recovering’ tile; land is never reallocated to the ‘unmanaged’ tile. The tiles are treated differently with respect to wildfire: on the ‘unmanaged’ and ‘recovering’ tiles, lightning-ignited wildfires are not suppressed, while fire is excluded from ‘managed’ tiles. For our analysis of total carbon (above and below ground), we only used the ‘recovering’ tile.

Climate data. Climate forcing used to drive LPJ-LMfire comes from the output of 13 GCMs in simulations produced for the CMIP6 Supplementary Table 2 (refs. 37,38). For each GCM, we obtained simulations for the historical period (1850–2014) and four future SSPs (SSP1-26, SSP2-45, SSP3-70 and SSP5-85 covering 2015–2100). We used only GCMs that archived all seven climate variables needed to run LPJ-LMfire: 2 m temperature (t_{as} , K), precipitation (pr , $\text{kg m}^{-2} \text{s}^{-1}$), convective precipitation (prc , $\text{kg m}^{-2} \text{s}^{-1}$), cloud cover (clt , %), minimum and maximum daily temperature (t_{min} , t_{max} , K), and 10 m surface wind speed (sfcWind , m s^{-1}) (Supplementary Fig. 2). For each model, we concatenated the historical simulation with a future scenario, calculated anomalies with respect to 1971–1990 and added those to observed 30 year climatologies to create bias-corrected monthly climate time series covering 1850–2100 (see Supplementary Information). Where multiple ensemble members were available from a GCM, we chose the first simulation.

Simulation protocol. We drove LPJ-LMfire with the GCM simulations described in the previous section, and the same atmospheric CO_2 concentrations and land use boundary conditions as those used in the CMIP6 simulations. All forcings cover the historical period (1850–2014) and the individual future SSPs (2015–2100). Each LPJ-LMfire simulation was initialized for 1,020 years with 1850 atmospheric CO_2 and land use, and the 1850s climatology of each CMIP6 GCM. This was followed by simulations with transient climate from 1850 to 2100 for each CMIP6 GCM under each of the four SSPs. For each of the 13 CMIP6 GCMs running each of the SSP scenarios, we conducted two CO_2 experiments (CO_2_{2014} and $\text{CO}_2_{\text{free}}$) and two fire experiments. In total, we ran 221 vegetation model simulations covering the range of future climate, CO_2 and fire scenarios.

Atmospheric CO_2 in these simulations either followed the CMIP6 historical and SSP trajectory for the entire 1850–2100 run ($\text{CO}_2_{\text{free}}$), or followed the historical CMIP6 trajectory until 2014, and was then fixed at 2014 concentrations for the remainder of the simulation (CO_2_{2014}). This allowed us to test the vegetation response to future climate change in the absence of additional CO_2 fertilization

of photosynthesis. Our simulations ended with the standard SSP projections in 2100, 80 years after restoration begins. We therefore could not assess the fate of restored carbon beyond that point. On the basis of the trends in the multi-model mean carbon uptake rates, we estimated that only under severe climate change will carbon storage be reduced shortly after 2100 in CO_2_{2014} .

In control simulations, land use followed the historical CMIP6 trajectory until 2014, after which it was fixed under 2014 conditions until 2100. Land use after 2014 was fixed at 2014 levels because it is the last year with common land use between all scenarios, which allowed us to identify future climate change impacts on restoration permanence and avoid influences from land abandonment and expansion prescribed in the different SSP scenarios.

In the restoration experiments, land use also followed the historical CMIP6 trajectory until 2014, but then diverged: cropland extent remained at 2014 levels until 2100, while pasture (or non-cropland land use) remained constant from 2014 to 2020 and was then linearly reduced by the restoration area from 2020 to 2030. From 2030, land use remained constant at that lower level until 2100. The amount of restoration in a grid cell was limited by the pasture area, that is, once all of the available pasture area had been restored, no additional restoration took place. Because it is highly unlikely to be practical to restore the entire target area of tropical forest at once, we linearly increased the restoration area from 2020 to 2030, which caused an expansion-driven increase in carbon uptake over the 11 year period (Extended Data Fig. 1). This means that two factors controlled carbon uptake over time in our experimental design: first the expansion of the restoration area, accounting for approximately 19.7 Pg C, and second the long-term effect of carbon accumulation (Extended Data Fig. 5).

Primary climate change impacts, such as drought and heat stress that reduce carbon uptake, were implicitly included in the climate forcing data, while secondary climate change impacts from wildfire were simulated by LPJ-LMfire on the basis of climate. To quantify the contribution of wildfire on the carbon storage from restoration, we repeated the simulations described above with fires turned off in LPJ-LMfire.

Restoration opportunity index. We created a restoration opportunity index to evaluate the suitability of locations for restoration on the basis of the ability for restoration to result in net carbon uptake over 2020–2100 and to store this carbon without episodes of major loss. For each of the 13 realizations of the four SSPs in the CO_2_{2014} experiment, we identified all restoration grid cells (1) that had a net carbon uptake by 2100 relative to 2030, and (2) where temporal reductions in total carbon storage over 2030–2100 were <10% of the 2030–2100 mean. For each simulation, grid cells meeting these criteria were then used to mask the rank sum of carbon uptake (grid cells ordered high to low) and opportunity cost (grid cells ordered low to high). We then summed this quantity across all 13 future simulations from the different GCMs, and standardized the resulting layer from 0–1. A score of 1 means that the restoration opportunity index is 1 under all future climate model simulations.

Data availability

The raw LPJ-LMfire model output and code for creating the figures in this manuscript are available at https://github.com/ARVE-Research/LPJ_futuretropics.

Code availability

The source code to run the version of LPJ-LMfire used for this research is archived at <https://doi.org/10.5281/zenodo.5831747>.

References

- Dinerstein, E. et al. An ecoregion-based approach to protecting half the terrestrial realm. *BioScience* **67**, 534–545 (2017).
- Sitch, S. et al. Evaluation of ecosystem dynamics, plant geography and terrestrial carbon cycling in the LPJ dynamic global vegetation model. *Glob. Change Biol.* **9**, 161–185 (2003).
- Kaplan, J. O. et al. Holocene carbon emissions as a result of anthropogenic land cover change. *Holocene* **21**, 775–791 (2010).
- Eyring, V. et al. Overview of the coupled model intercomparison project phase 6 (CMIP6) experimental design and organization. *Geosci. Model Dev.* **9**, 1937–1958 (2016).
- O’Neill, B. C. et al. The scenario model intercomparison project (scenariomip) for CMIP6. *Geosci. Model Dev.* **9**, 3461–3482 (2016).

Acknowledgements

We thank K. H.-K. Lau for assistance in plotting the figures in this paper; the World Climate Research Programme which, through its Working Group on Coupled Modelling, coordinated and promoted CMIP6; the climate modelling groups for producing and making available their model output; the Earth System Grid Federation (ESGF) for archiving the data and providing access; the multiple funding agencies that support

CMIP6 and ESGF; the TRENDY modelling groups for producing and making available their DGVM output; and the FLUXCOM initiative for providing GPP data.

Author contributions

A.K. and J.O.K. conceived and designed the study. A.K. performed the simulations and analysed the results in consultation with J.O.K. Both authors contributed to the writing of the manuscript.

Competing interests

The authors declare no competing interests.

Additional information

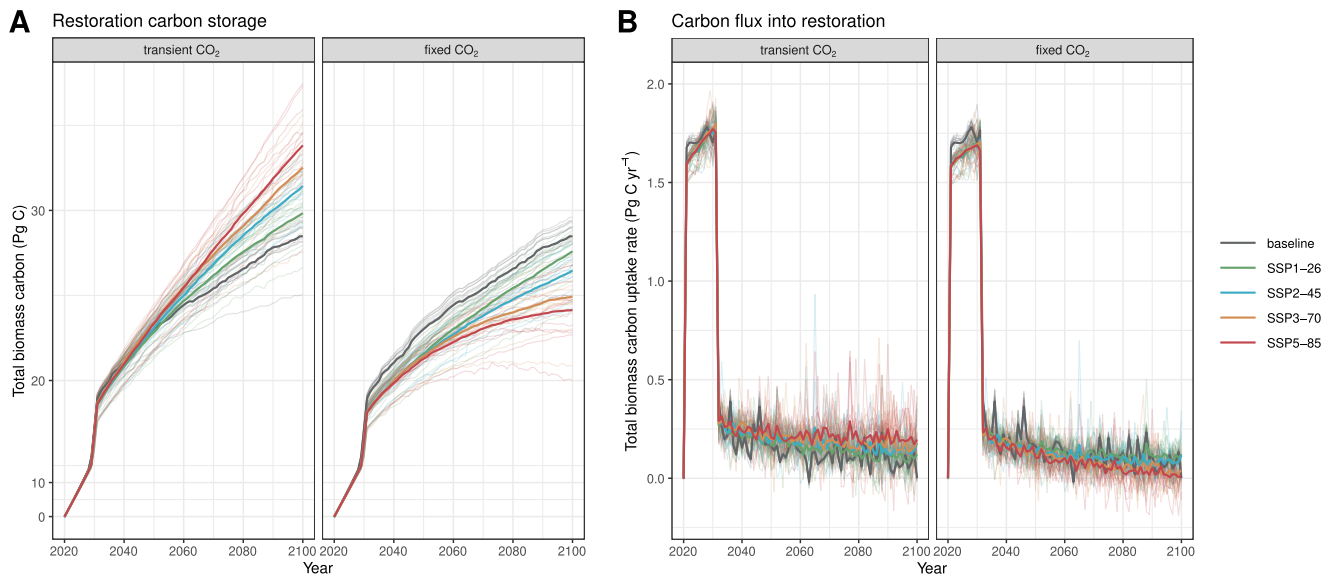
Extended data is available for this paper at <https://doi.org/10.1038/s41558-022-01289-6>.

Supplementary information The online version contains supplementary material available at <https://doi.org/10.1038/s41558-022-01289-6>.

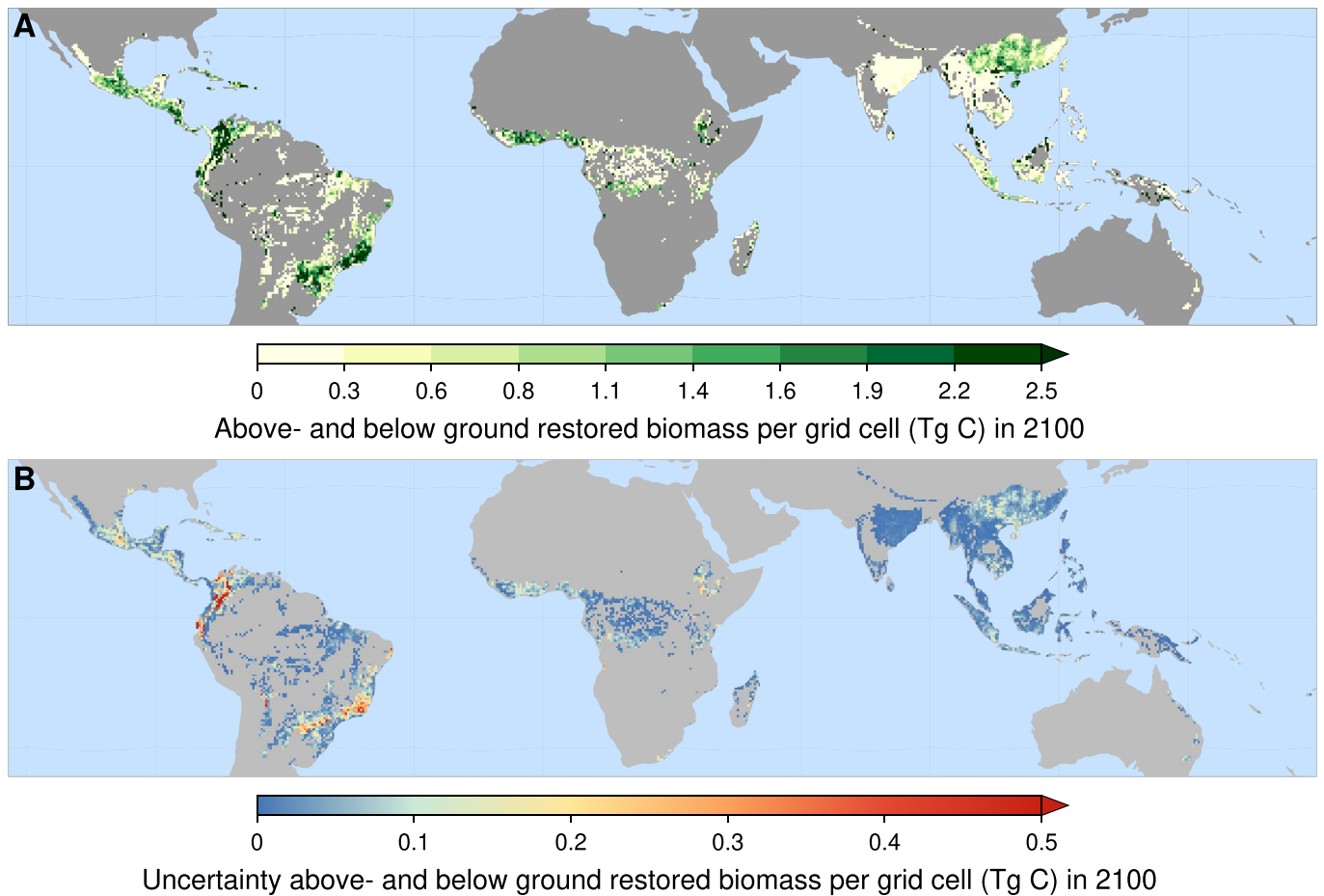
Correspondence and requests for materials should be addressed to Alexander Koch or Jed O. Kaplan.

Peer review information *Nature Climate Change* thanks Nima Madani and the other, anonymous, reviewer(s) for their contribution to the peer review of this work.

Reprints and permissions information is available at www.nature.com/reprints.

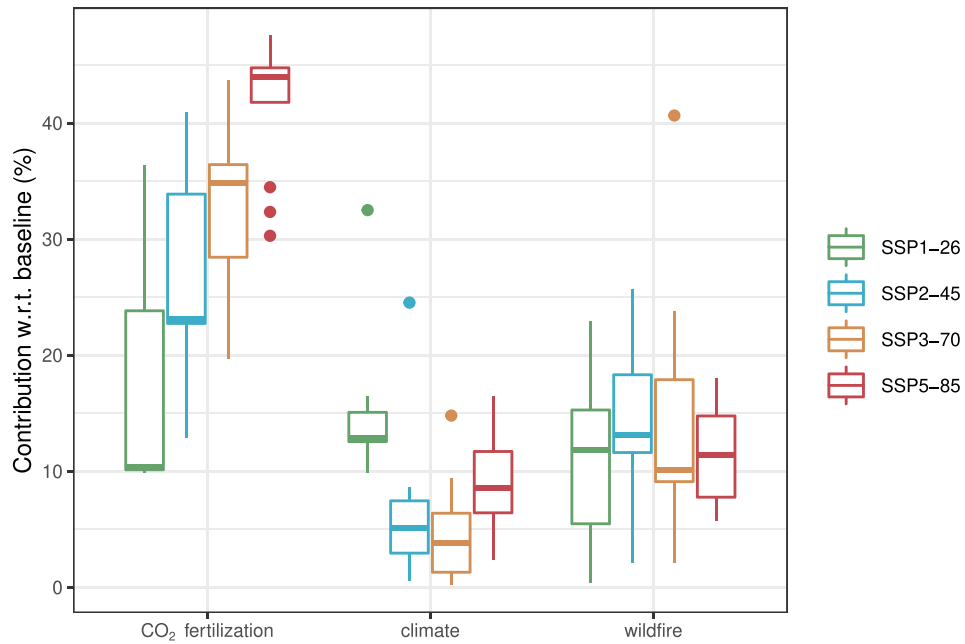


Extended Data Fig. 1 | Time series of carbon accumulation from tropical forest restoration over time under different scenarios. Cumulative total carbon gain A and annual total carbon gain B from tropical forest restoration (2020–2100) under different climate change scenarios (SSPs) with unconstrained (left, $CO_{2,free}$) and limited CO_2 fertilization (right, $CO_{2,2014}$). Note the nonlinear y-axes in A (0–10 Pg C).

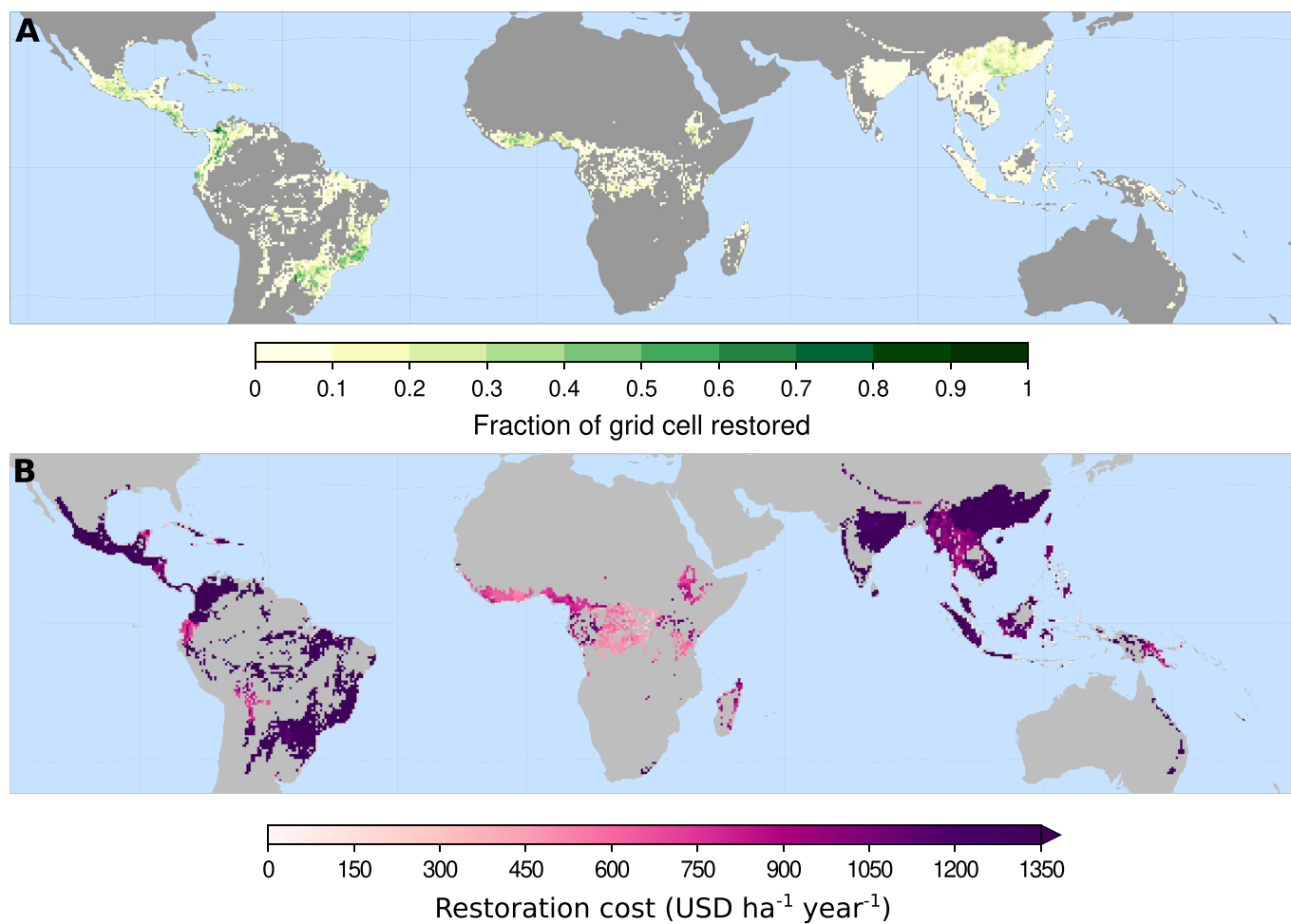


Extended Data Fig. 2 | Carbon gain from tropical forest restoration by 2100. Multi-model A mean and B standard deviation (CMIP6 climate drivers) of total carbon gain per grid cell from restoration (2020-2100) under SSP2-45 with limited CO₂ fertilization and no fire management. Carbon gain is difference in the living above- and below ground biomass for 2100 of the restoration scenario and the control scenario with no-restoration (that is 2014 land use and 2100 climate).

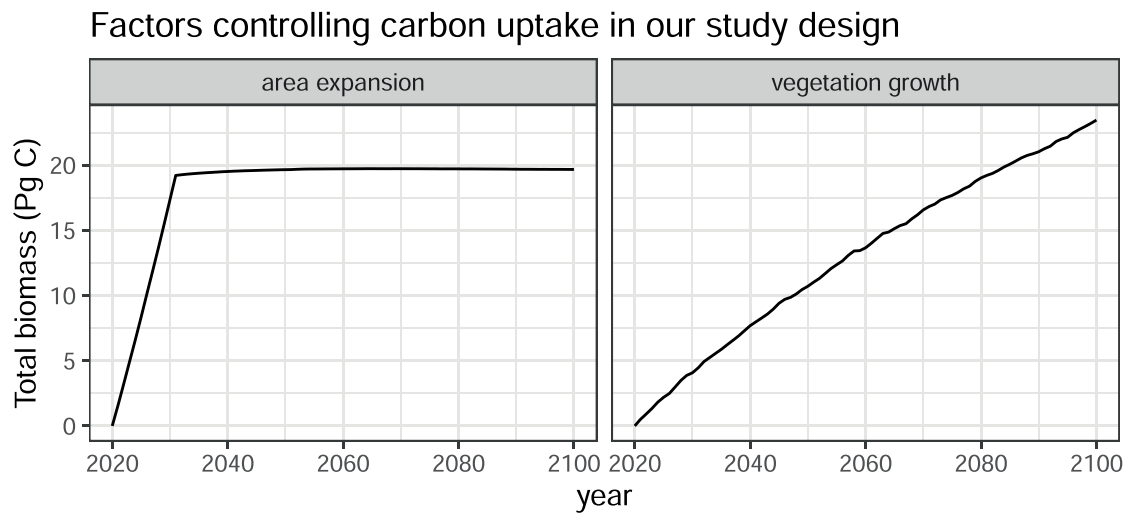
Contribution of CO₂ fertilization, climate change, and wildfire to uncertainty in carbon uptake



Extended Data Fig. 3 | Contribution of CO₂ fertilization, climate change, and wildfires to changes in carbon storage from restoration by 2100 under four future climate change scenarios. Each sample is based on the climate of one potential realization of a SSP scenario simulated by one of 13 CMIP6 models. Boxplots representing 25th, 50th, and 75th quantile, whiskers are the 5th and 95th quantile and individual points are outliers.



Extended Data Fig. 4 | Spatial distribution of A restored land and B restoration cost. Fraction of grid cells under restoration based on the restorable area from² and the non-cropland land use extent in 2014 based on CMIP6 historical forcing³⁷. Restoration cost based on cost of land, labour, and restoration management following²⁷.



Extended Data Fig. 5 | Factors determining increase in biomass carbon in our experiment. The increase in total living above- and below ground biomass is determined by the gradual expansion in restoration area (2020-2030) and the re-growth of natural vegetation on the restored area (2020-2100). Carbon accumulation is based on climate forcing from MPI-ESM1-2-HR under the SSP2-45 scenario with $CO_{2,free}$.